

High-frequency hopping conductivity in the quantum Hall effect regime: Acoustical studies

I. L. Drichko,¹ A. M. Diakonov,¹ I. Yu. Smirnov,¹ Yu. M. Galperin,^{1,2} and A. I. Toropov³

¹*A. F. Ioffe Physico-Technical Institute of Russian Academy of Sciences, Polytechnicheskaya 26, 194021 St. Petersburg, Russia*

²*Centre for Advanced Studies, Drammensveien 78, 0271 Oslo, Norway*

and Department of Physics, University of Oslo, P.O. Box 1048 Blindern, 0316 Oslo, Norway

³*Semiconductors Physics Institute of Siberian Division of Russian Academy of Sciences, Akademika Lavrentieva 13, 630090 Novosibirsk, Russia*

(Received 6 March 2000)

The high-frequency conductivity of Si δ -doped GaAs/AlGaAs heterostructures is studied in the integer quantum Hall effect (QHE) regime, using acoustic methods. Both the real and the imaginary parts of the complex conductivity are determined from the experimentally observed magnetic field and temperature dependencies of the velocity and the attenuation of a surface acoustic wave. It is demonstrated that in structures with carrier density $(1.3-2.8) \times 10^{11} \text{ cm}^{-2}$ and mobility $(1-2) \times 10^5 \text{ cm}^2/\text{V s}$ the mechanism of low-temperature conductance near the QHE plateau centers is hopping. It is also shown that at magnetic fields corresponding to filling factors 2 and 4, the doped Si δ layer efficiently shunts the conductance in the two-dimensional electron gas (2DEG) channel. A method to separate the two contributions to the real part of the conductivity is developed, and the localization length in the 2DEG channel is estimated within the context of a nearest-neighbor hopping model.

I. INTRODUCTION

It is well known from numerous low-temperature resistivity measurements that the electronic states of a two-dimensional electron gas (2DEG) whose energies are located between two adjacent Landau levels in a perpendicular magnetic field, are localized. Consequently, the conductance is determined by electron hopping between the localized states. The hopping mechanism is temperature dependent. At temperatures 1-4 K, the conductance σ is usually determined by nearest-neighbor hopping. In this case its temperature dependence is mainly exponential, $\sigma_{xx}(T) \propto \exp(-E/kT)$ where E is the temperature-independent activation energy, see e.g., Refs. 1-3 and references therein. (We assume that the 2DEG is located in the $x-y$ plane, the magnetic field is parallel to the z axis, and the electric field is along the x axis.) At lower temperatures, $T \leq 1$ K, the electron hopping distance appears to be greater than the typical distance between nearest neighbors: at such low temperatures it becomes difficult to find a neighbor whose energy is close to the initial one within the accuracy kT . In this so-called *variable-range-hopping* regime the conductivity σ_{xx} is also exponentially small,^{2,4-6} but with an effective activation energy E , which is temperature-dependent.

To clarify the nature of the localized states, we study in this paper the two-dimensional *high-frequency* (hf) conductance of a 2DEG, $\sigma_{xx}(\omega)$, by measuring the velocity and the attenuation of surface acoustic waves (SAW) propagating along the x direction nearby the electron layer. Acoustic methods are particularly promising for our task since $|\sigma_{xx}(\omega)|$ in the hopping regime may be of the same order of magnitude as the SAW velocity V . Because the screening of the electric fields produced by the SAW is determined by the ratio σ_{xx}/V , the acoustic properties are sensitive to the variations in σ_{xx} . Furthermore, the attenuation and the velocity of the SAW depend on the *complex* conductance,

$$\sigma_{xx}(\omega) \equiv \sigma_1(\omega) - i\sigma_2(\omega),$$

and hence both the active σ_1 and the reactive σ_2 components can be detected. The active component can be then compared to the static conductivity σ_{dc} . A pronounced difference will clearly indicate that the electron states are localized. We compare the experimental results for $\sigma_1(\omega)$ and $\sigma_2(\omega)$ with existing models for the dielectric response of localized states and extract relevant parameters of the latter.

The paper is organized as follows. In Sec. II the experimental setup is presented. Experimental results and their discussion are given in Sec. III. They are summarized in Sec. IV. Details of the derivation of the expressions we use are presented in the Appendix.

II. THE EXPERIMENTAL SETUP

A sketch of the experimental setup is shown in Fig. 1. A SAW propagating along the surface of a piezoelectric crystal is accompanied by a wave of hf electric field. This electric field penetrates into a 2DEG located in a semiconductor heterostructure mounted on the surface. The field produces electrical currents which, in turn, cause Joule losses. As a result, there are electron-induced contributions both to the SAW attenuation and to its velocity. These effects are governed by the complex frequency-dependent conductivity, $\sigma_{xx}(\omega)$,

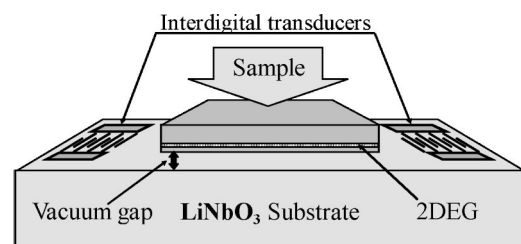


FIG. 1. The experimental setup.

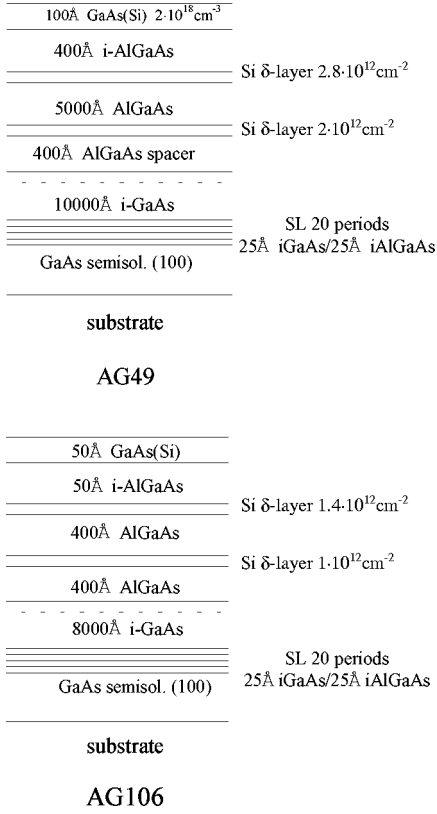


FIG. 2. The structures of the samples AG49 and AG106.

which oscillates as a function of the external magnetic field. Hence, specific oscillations will appear both in the SAW attenuation and its velocity. Under reasonable assumptions, the experimental results allow one to determine $\sigma_{xx}(\omega)$ as function of the magnetic field and to analyze its properties. In the present paper, the attenuation coefficient Γ and the relative velocity change, $\Delta V/V$, are measured as functions of perpendicular magnetic field up to 7 T in the temperature interval 1.5–4.2 K. The Si δ -doped GaAs/AlGaAs heterostructure samples with sheet densities $n = (1.3 - 2.7) \times 10^{11} \text{ cm}^{-2}$ and mobilities $\mu = (1 - 2) \times 10^5 \text{ cm}^2/\text{Vs}$ at $T = 4.2 \text{ K}$ were grown by molecular-beam epitaxy, their structures being shown in Fig. 2.

III. EXPERIMENTAL RESULTS AND THEIR DISCUSSION

The expressions relating Γ and $\Delta V/V$ to the complex conductance, $\sigma_1 - i\sigma_2$, can be extracted from Refs. 7 and 8. They read

$$\Gamma \text{ (dB/cm)} = 4.34 AK^2 k \gamma, \quad (1)$$

$$\Delta V/V = (AK^2/2) (\delta v/v). \quad (2)$$

Here $k = \omega/V$ is the SAW wave vector, K^2 is the piezoelectric coupling constant of the substrate (Y-cut LiNbO₃), and

$$A = 8b(k)(\epsilon_1 + \epsilon_0)\epsilon_0^2\epsilon_s e^{-2k(a+d)}, \quad (3)$$

$$b(k) = \{b_1(k)[b_2(k) - b_3(k)]\}^{-1}, \quad (4)$$

$$b_1(k) = (\epsilon_1 + \epsilon_0)(\epsilon_s + \epsilon_0) - (\epsilon_1 - \epsilon_0)(\epsilon_s - \epsilon_0)e^{(-2ka)}, \quad (5)$$

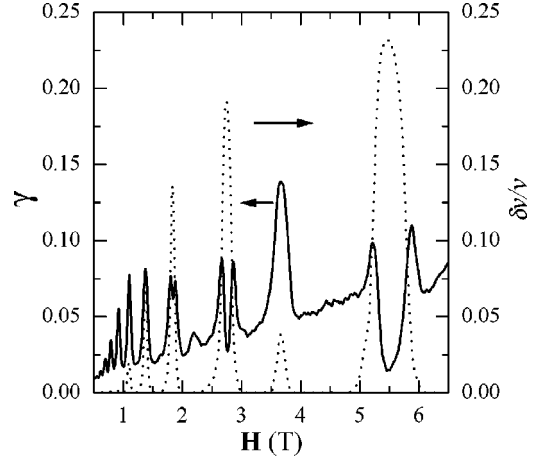


FIG. 3. The experimental dependencies of the reduced SAW attenuation, γ and reduced SAW velocity variation, $\delta v/v$, on the perpendicular magnetic field H . $T = 1.5 \text{ K}$, $f = 30 \text{ MHz}$.

$$b_2(k) = (\epsilon_1 + \epsilon_0)(\epsilon_s + \epsilon_0) + (\epsilon_1 - \epsilon_0)(\epsilon_s - \epsilon_0)e^{(-2kd)}, \quad (6)$$

$$b_3(k) = (\epsilon_1 - \epsilon_0)(\epsilon_s - \epsilon_0)e^{(-2ka)} + (\epsilon_1 - \epsilon_0) \times (\epsilon_s + \epsilon_0)e^{[-2k(a+d)]}. \quad (7)$$

In these equations, $\epsilon_1 = 50$, $\epsilon_0 = 1$, and $\epsilon_s = 12$ are the dielectric constants of LiNbO₃, of the vacuum and of the semiconductor, respectively. a is the finite vacuum clearance between the sample surface and the LiNbO₃ surface and d denotes the finite distance between the sample surface and the 2DEG layer. In our experiment, the heterostructure was pressed to the piezoelectric platelet. Even in this case the clearance a remains finite because of some roughness of both surfaces. Since the actual clearance is hardly controlled, we treat a as an adjustable parameter. The quantity a is determined by fitting the experimental data in the region of metallic conductivity where the complex conductivity is essentially frequency independent at our frequencies (30–210 MHz). The values of a are slightly different for different sample setups. We have checked that for a given setup the values of σ_{xx} extracted in this way are indeed frequency independent in the above-mentioned range of magnetic fields. More details regarding the fitting procedure are given in Ref. 9.

The parameters of our experimental setup are $a = 0.5 \mu\text{m}$ and $d = 0.59 \mu\text{m}$ for the first sample, and $0.09 \mu\text{m}$ for the second one. The reduced attenuation γ and velocity variation $\delta v/v$ are given by the expressions

$$\gamma = \frac{\Sigma_1}{\Sigma_1^2 + (1 + \Sigma_2)^2}, \quad \delta v/v = \frac{1 + \Sigma_2}{\Sigma_1^2 + (1 + \Sigma_2)^2}; \quad (8)$$

$$\Sigma_i = (4\pi\sigma_i/\epsilon_s V) t(k), \quad t(k) = [b_2(k) - b_3(k)]/2b_1(k).$$

The experimental magnetic-field dependence of γ and $\delta v/v$ for the sample with carrier density $n = 2.7 \times 10^{11} \text{ cm}^{-2}$ and mobility $\mu = 2 \times 10^5 \text{ cm}^2/\text{Vs}$ are shown in Fig. 3. Similar results have been found previously in GaAs/AlGaAs heterostructures.¹⁰

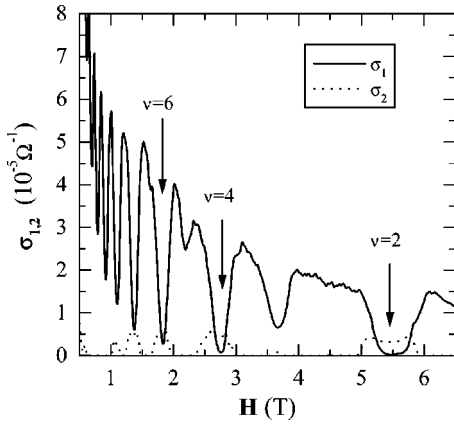


FIG. 4. The experimental dependencies of real σ_1 and imaginary σ_2 parts of high-frequency conductivity of a 2DEG on the perpendicular magnetic field H . $T=1.5$ K, $f=30$ MHz.

The real and the imaginary parts of the complex conductivity are derived from Γ and $\Delta V/V$, using Eqs. (1) and (2). The results obtained for $T=1.5$ K and acoustic frequency 30 MHz are shown in Fig. 4.

As can be seen, σ_2 practically vanishes near half-integer filling factors, i.e., when the Fermi level is close to any Landau level. In such regions $\sigma_1(\omega)$, as has been shown in Ref. 11, appears to be close to the static conductivity σ_{dc} . These facts indicate that the electron states are indeed *extended*. With a further increase of the magnetic field the Fermi level leaves the Landau band, a metal-dielectric transition takes place, and the electrons become localized in the randomly fluctuating potential of the charged impurities.

As the Fermi level departs from the Landau-level center, $\sigma_1(\omega)$ becomes clearly larger than σ_{dc} , see Fig. 5. Such a behavior can be qualitatively interpreted¹¹ as absorption by large clusters (“lakes”) disconnected from each other. Inside each cluster the absorption is determined by the value of σ_{dc} . Since the area occupied by the clusters is less than the area occupied by the infinite cluster at the mobility edge, the effective $\sigma_1(\omega)$ is less than σ_{dc} at half-integer ν . At the same time, $\sigma_1(\omega)$ is greater than σ_{dc} in the same magnetic

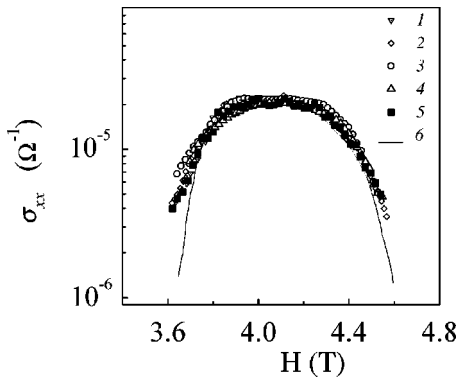


FIG. 5. DC-measured conductivity of a 2DEG σ_{dc} (solid line) and acoustically-measured hf conductivity of a 2DEG $\sigma_1(\omega)$ versus magnetic field H in the region close to the fourth Landau-level center. The symbols correspond to frequencies f (MHz) and vacuum gap widths a (μm): (1) 213 and 0.3, (2) 30 and 0.5, (3) 150 and 0.3, (4) 30 and 0.4, (5) 90 and 1.2. $T=4.2$ K, the electron density is $n=7 \times 10^{11} \text{ cm}^{-2}$.

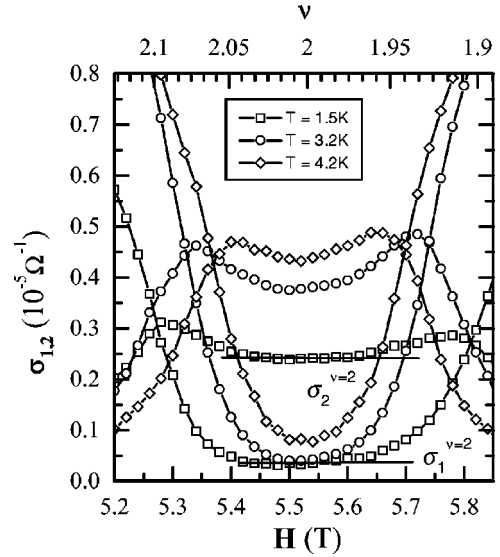


FIG. 6. Magnetic-field dependencies of real part $\sigma_1(\omega)$ and imaginary part $\sigma_2(\omega)$ of hf conductivity of a 2DEG near the filling factor $\nu=2$ at $T=1.5-4.2$ K, $f=\omega/2\pi=30$ MHz for the sample with $n=2.7 \times 10^{11} \text{ cm}^{-2}$ (AG49).

field because there is no infinite conducting cluster at the Fermi level. The imaginary part, $\sigma_2(\omega)$ *increases* as the Fermi level departs from the Landau-level’s center.

At magnetic fields corresponding to small integer filling factors, when the Fermi level finds itself in-between the adjacent Landau levels, where $\sigma_{dc} \approx 0$, $\sigma_2(\omega)$ becomes about an order of magnitude larger than σ_1 , see Fig. 6. Figure 7 depicts the temperature dependencies of $\sigma_1(\omega)$ at $f=30$ MHz in magnetic fields corresponding to the midpoints of the Hall plateaus. One can see a crossover from a smooth temperature dependence at a strong magnetic field (5.5 T), to a rather steep increase with temperature at weaker fields. Such behavior is compatible with the idea that the conduc-

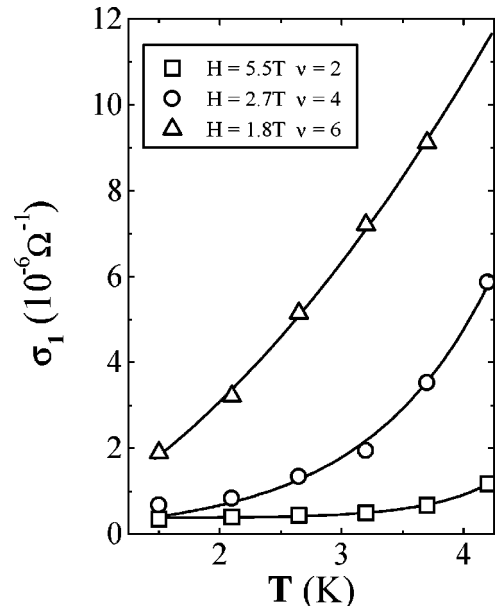


FIG. 7. Temperature dependencies of real part $\sigma_1(\omega)$ of hf conductivity of a 2DEG at $f=30$ MHz in magnetic fields corresponding to integer filling factors.

tivity consists of two contributions. The first one is due to the extended states near the adjacent upper Landau level, while the second is coming from the localized states at the Fermi level.¹² The relative occupation of the extended states increases with increasing temperature because of thermally activated processes. Obviously, this effect is dominant at small magnetic fields.

We now turn to the region of low temperatures and filling factors close to 2, where hopping between the localized states gives the main contribution to dielectric response. To analyze the experimental results we adopt the so-called *two-site approximation*, according to which an electron hops between states with close energies localized at two different impurity centers. These states form *pair complexes* which do not overlap. Therefore, they do not contribute to the static conductivity but are important for the ac response. Being very simple, the two-site model has been extensively studied, see for a review Refs. 13–15 and references therein. In the following we will use the 2D version of the theory.¹³ Some details of the discussion depend on the assumptions regarding both the density of localized states and the relaxation mechanisms of their population. We therefore rederive the theoretical results in Appendix A.

As is well known,¹⁴ there are two specific contributions to the high-frequency absorption. The first contribution, the so-called *resonant*, is due to direct absorption of microwave quanta accompanied by interlevel transitions. The second one, the so-called *relaxational*, or *phonon assisted*, is due to phonon-assisted transitions, which lead to a lag of the levels populations with respect to the microwave-induced variation in the interlevel spacing. The relative importance of the two mechanisms depends on the frequency ω , the temperature T , as well as on sample parameters. The most important of them is the relaxation rate $\gamma_0(T)$ of *symmetric* pairs with interlevel spacing $E = kT$. At $\omega \lesssim \sqrt{kT\gamma_0/\hbar}$ the relaxation contribution to $\sigma_1(\omega)$ dominates, and only this one will be taken into account. Following the derivation given in Appendix A we obtain

$$\sigma_1 = \frac{\pi^2}{2} \frac{g^2 \xi^3 \omega e^4}{\epsilon_s} (\mathcal{L}_T + \mathcal{L}_\omega/2)^2. \quad (9)$$

Here g is the (constant) single-electron density-of-states at the Fermi level, ξ is the localization length of the electron state, $\mathcal{L}_T = \ln J/kT$, J is a typical value of the energy overlap integral, which is of the order of the Bohr energy, while $\mathcal{L}_\omega = \ln(\gamma_0/\omega)$. Equation (9) is valid provided that the logarithmic factors are large. Note that the product $r_\omega = \xi(\mathcal{L}_T + \mathcal{L}_\omega/2)$ is the distance between the sites forming a hopping pair. Note also that Eq. (9) is similar to the result obtained in Ref. 13, but differs from it by some logarithmic factors and a numerical factor of 1/4.

The analysis of $\sigma_2(\omega)$ is a bit more complicated because virtual zero-phonon transitions give a comparable contribution. The analysis presented in the Appendix leads to the following expression for the ratio $\sigma_2(\omega)/\sigma_1(\omega)$,

$$\frac{\sigma_2}{\sigma_1} = \frac{2\mathcal{L}_\omega(\mathcal{L}_T^2 + \mathcal{L}_T\mathcal{L}_\omega/2 + \mathcal{L}_\omega^2/12) + 4c\mathcal{L}_T^2\mathcal{L}_\omega}{\pi(\mathcal{L}_T^2 + \mathcal{L}_T\mathcal{L}_\omega + \mathcal{L}_\omega^2/4)}. \quad (10)$$

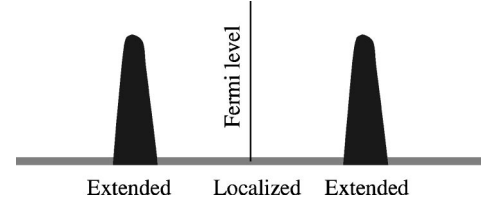


FIG. 8. Schematic profile of the single-electron density-of-states.

Here $\mathcal{L}_c = \ln(\hbar\omega_c/kT)$, ω_c is the cyclotron frequency, and $c \gtrsim 1$ is a numerical factor depending on the density-of-states in the region between the Landau levels, see the Appendix. Using the estimate for γ_0 from Ref. 15,

$$\gamma_0 = \frac{4\pi e^2 K^2 kT}{\epsilon_s \hbar^2 V},$$

valid for the piezoelectric relaxation mechanism, as well as other parameters relevant to the present experiment, one concludes that in the hopping regime $\sigma_2 \gtrsim \sigma_1$. This conclusion agrees with the experimental results obtained for the middles of the Hall plateaus at 5.5 T and 2.7 T and ensures that the conductance mechanism in these regions is indeed hopping.

Given an experimental value for σ_1 , one can obtain from Eq. (9) the localization length ξ provided that the single-electron density-of-states g is known for given values of the magnetic field. This quantity has been obtained from the temperature-dependence measurements of the thermally activated dc conductivity.¹³ It has been shown that for small filling factors the density-of-states in the plateau regions is finite and almost field independent, see Fig. 8. Using the density-of-states versus mobility curve from Ref. 1, obtained for a sample similar to ours, we estimate the density-of-states as $g = 2.5 \times 10^{24} \text{ cm}^{-2} \text{ erg}^{-1}$. On the other hand, according to Ref. 3, the density-of-states as function of the magnetic field H can be expressed by the interpolation formula

$$g(H) = \frac{g_0}{1 + \sqrt{\mu H}}, \quad (11)$$

where μ is the mobility of the 2D electrons while $g_0 = m/(\pi\hbar^2)$ is the 2D density-of-states at $H=0$. From Eq. (11) we obtain for $H=5.5$ T the density-of-states $g = 1.7 \times 10^{24} \text{ cm}^{-2} \text{ erg}^{-1}$.

Using the first estimate for the density-of-states one obtains $\xi = 6.5 \times 10^{-6} \text{ cm}$, that is about 1.6 times greater than the spacer thickness $l_{\text{sp}} = 4 \times 10^{-6} \text{ cm}$. On the other hand, it is the spacer width that characterizes the random potential correlation length in the 2DEG layer. Hence, this fact contradicts our interpretation of experimental results in terms of pure nearest-neighbor pair hopping.

To improve the agreement with the two-site hopping model, we assume that the high-frequency hopping conductivity of the 2DEG channel is shunted by hopping along the doping Si δ layer. This assumption can be substantiated as follows. Let us suppose that at the middle of the Hall plateau $\sigma_1^{\nu=2} = 4 \times 10^{-7} \Omega^{-1}$ and $\sigma_2^{\nu=2} = 2.4 \times 10^{-6} \Omega^{-1}$ are entirely determined by the hopping conductivity along the Si δ layer. Such a contribution is only weakly dependent on the magnetic field because the latter is too weak to deform sig-

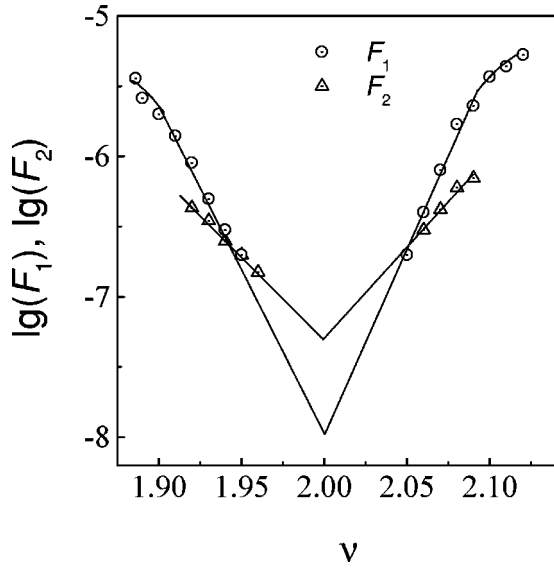


FIG. 9. The dependences of $\log(F_1)=\log(\sigma_1-\sigma_1^{\nu=2})$ and $\log(F_2)=\log(\sigma_2-\sigma_2^{\nu=2})$ versus the filling factor ν near $\nu=2$. $T=1.5$ K, $f=30$ MHz. Note that both extrapolated curves show a cusp in the middle of the plateau.

nificantly the wave functions of the Si dopants. Then the contributions to σ_i associated with the 2DEG channel are just the difference between the experimentally measured σ_i in a given magnetic field and its value at $\nu=2$.

We now analyze the dependence of the differences $F_1 \equiv \sigma_1 - \sigma_1^{\nu=2}$ and $F_2 \equiv \sigma_2 - \sigma_2^{\nu=2}$ on the filling factor ν . The plots of $\log F_i$ versus ν are shown in Fig. 9. Both curves approach straight lines, and consequently can be extrapolated to $\nu=2$. Using this extrapolation we have obtained $F_1^{\nu=2} = 10^{-8} \Omega^{-1}$ and $F_2^{\nu=2} = 5 \times 10^{-8} \Omega^{-1}$. It should be noticed here that the extrapolated values of $F_i^{\nu=2}$ are two orders of magnitude smaller than the values of $\sigma_i^{\nu=2}$, associated with the hopping along the Si- δ -layer. Using the extrapolated values of F_1 and F_2 to extract the 2DEG contributions to σ_1 and σ_2 , one can calculate the electron localization length at $\nu=2$ from Eq. (9). This procedure is corroborated by the fact that the experimental ratio $F_2/F_1=5$ is close to the theoretical value 4.2 coming from Eq. (10). The localization length at $\nu=2$ obtained in this way is $\xi=2 \times 10^{-6}$ cm, which is half of the spacer width. This estimate makes realistic the ‘‘two-site model,’’ which we have extensively used. It should be emphasized, however, that from the above value of ξ , the hopping length r_ω is estimated to be 1.4×10^{-5} cm. Consequently, there is an interplay between hops to the nearest and more remote neighbors. A more rigorous theory for this situation should be worked out. Such a theory should also explain why the magnetic-field dependencies of σ_1 and σ_2 at the vicinity of $\nu=2$ appear to be different—the $\sigma_1(H)$ dependence is more pronounced than the $\sigma_2(H)$ one. According to the two-site model, both are determined by the respective dependence of the localization length on the magnetic field and should be similar. Indeed, their ratio, from Eq. (10), is almost field independent. It follows from the experimental data that there exists an additional mechanism leading to the pronounced decrease of σ_2 as the Fermi level falls into the extended states region. A probable mechanism is thermal activation of electrons from the Fermi level to the

upper Landau band, leading, first, to a decrease of the number of pairs responsible for the hopping conductivity, and, second to a screening of the electric-field amplitude produced by the SAW. We hope to work out a proper quantitative theory in the future.

IV. CONCLUSIONS

The above analysis leads to the following conclusions:

(1) At the vicinity of the Hall plateau centers, high-frequency hopping conductance in the 2DEG layer can be effectively shunted by hopping inside the doping δ layer.

(2) When the shunting effect is properly subtracted, the results appear to be compatible with the nearest-neighbor two-site model of hopping conductivity.

(3) The localization length determined at different magnetic fields (and, consequently, different filling factors) by the above method, scales as the magnetic length $a_H = (\hbar/eH)^{1/2}$. This agrees with the concept of nearest-neighbor hopping.

(4) The interpretation of the imaginary part of the conductivity $\sigma_2(\omega)$, appears more complicated. While the magnetic-field dependence of the real part of the hf hopping conductivity of 2D electrons seems to be determined by the magnetic-field dependence of the localization length—the slope of $\log \xi(H)$, calculated from the values of $F_1^{\nu=2}(H)$ using Eq. (9), is close to the slope of $\log \xi(H)$ in Ref. 2—the magnetic-field dependence of the imaginary part of the hf conductivity has been explained so far only qualitatively. A more detailed quantitative analysis, which would include a proper account of the screening of the SAW-induced hf electrical field by both layers, is required.

It is worth emphasizing that the acoustic method used in the present paper allows the determination of the localization length near the Hall plateau centers. This is very difficult to achieve using a dc technique.

ACKNOWLEDGMENTS

The work has been supported by RFFI No 98-02-18280 and MNTRF N 97-1043 grants. One of the authors, I.L.D., has also received a support by the Research Council of Norway. We are grateful to Ora Entin-Wohlman.

APPENDIX: DERIVATION OF $\sigma(\omega)$

The derivations of the complex $\sigma(\omega)$ within the two-site approximation have been extensively discussed, see e.g., Refs. 14 and 15. However, the resulting formulas differ in some details. These differences are mainly due to different assumptions about the relaxation of the occupation numbers of the localized states. We therefore present here a unified derivation, in order to clarify the various assumptions and notations.

Let us characterize the sites by the single-electron energies $\varphi_{1,2}$, which would be the actual energies if the Coulomb correlation between the occupation numbers is ignored. The two electron energies, in the absence of quantum hybridization of the states, can be specified by four terms,

$$W_0=0, \quad W_1=\varphi_1, \quad W_2=\varphi_2, \quad W_3=\varphi_1+\varphi_2+\frac{e^2}{\epsilon_s r}.$$

Here r is the distance between the sites. As shown in Ref. 14, when the frequency ω and the temperature T are low enough, such that $\hbar\omega, kT \ll e^2/\varepsilon_s r$, only the two terms W_1 and W_2 can be occupied, and we face a situation of a two-level electronic system. Quantum tunneling hybridizes the two levels, so that the resulting energies are

$$W_{\pm} = \frac{\varphi_1 + \varphi_2}{2} \pm \frac{E}{2}, \quad E = \sqrt{\Delta^2 + \Lambda^2(r)}.$$

Here $\Delta = \varphi_1 - \varphi_2$, $\Lambda(r)$ is the energy overlap integral that decays as r increases. The effective Hamiltonian corresponding to this situation is

$$\mathcal{H}_{LR} = \frac{1}{2} \begin{pmatrix} \Delta & -\Lambda \\ -\Lambda & -\Delta \end{pmatrix} = \frac{1}{2} (\Delta \sigma_z - \Lambda \sigma_x). \quad (\text{A1})$$

Here σ_i are the Pauli matrices. Diagonalizing this Hamiltonian we obtain $\mathcal{H}_0 = (E/2) \sigma_z$.

The quantities φ_i are random, and their distributions are specified as follows.¹⁴ The ‘‘center-of-gravity’’ $(\varphi_1 + \varphi_2)/2$ is assumed to be uniformly distributed within a band of width $e^2/\varepsilon_s r$; and the difference $\Delta \equiv \varphi_1 - \varphi_2$, is also assumed to be uniformly distributed within a band much wider than kT . Since $d^2r = r dr d\phi$, where ϕ is the polar angle in the 2DEG plane, we obtain an r -independent pair distribution function $\mathcal{P}(\Delta, r, \phi) = g^2 e^2/\varepsilon_s$, where g is the (constant) single-electron density-of-states. It is convenient to change the variables from Δ, r, ϕ to Δ, Λ, ϕ ,

$$\mathcal{P}(\Delta, \Lambda, \phi) = g^2 (e^2/\varepsilon_s) |dr_{\Lambda}/d\Lambda|, \quad (\text{A2})$$

where r_{Λ} is the solution of the equation $\Lambda(r) = \Lambda$.

In the presence of an external ac electric field \mathbf{E} the pair acquires a dipole moment $\hat{\mathbf{d}} = e\hat{\mathbf{r}}$, described by the interaction Hamiltonian $\mathcal{H}_i = (\mathbf{E} \cdot \hat{\mathbf{d}}) = e(\mathbf{E} \cdot \hat{\mathbf{r}})$. This interaction is added to Δ in the Hamiltonian (A1). In the representation where \mathcal{H}_0 is diagonal, the interaction Hamiltonian becomes

$$\mathcal{H}_{\text{int}} = e(\mathbf{E} \cdot \hat{\mathbf{r}}) \left(\frac{\Delta}{E} \sigma_z - \frac{\Lambda}{E} \sigma_x \right). \quad (\text{A3})$$

The contribution of a pair to the complex $\sigma(\omega)$ can be expressed in terms of the complex susceptibility, $\chi(\omega) = \sigma(\omega)/i\omega$, which in turn is given by (cf. Ref. 16)

$$\chi(\omega) = \frac{\pi e^4 g^2}{\varepsilon_s} \int d\Delta d\Lambda r_{\Lambda}^2 |dr_{\Lambda}/d\Lambda| \times [(\Delta/E)^2 \chi_{zz}(\omega) + (\Lambda/E)^2 \chi_{xx}(\omega)]. \quad (\text{A4})$$

The partial susceptibilities χ_{pq} are given by (cf. Ref. 16)

$$\chi_{zz} = \frac{1}{kT \cosh^2(E/2kT)} \frac{i\gamma_{\parallel}}{\omega + i\gamma_{\parallel}}, \quad (\text{A5})$$

$$\chi_{xx} = \tanh\left(\frac{E}{2kT}\right) \sum_{\pm} \mp \frac{\hbar^{-1}}{\omega \mp E/\hbar + i\gamma}, \quad (\text{A6})$$

where γ and γ_{\parallel} are the proper relaxation rates. χ_{zz} is responsible for the relaxational contribution, while χ_{xx} is responsible for the resonant one.

To continue the calculations one needs to specify the spatial dependence of the overlap integral. Let us assume that $\Lambda(r) = J e^{-r/\xi}$, where ξ is the localization length. Then, $r_{\Lambda} = \xi \ln(J/\Lambda)$, $|dr_{\Lambda}/d\Lambda| = \xi/\Lambda$. At the next step, it is convenient to transform the variables from Δ, Λ to $E, p = (\Lambda/E)^2$, the Jacobian being $(2p)^{-1}(1-p)^{-1/2}$. This results in

$$\tilde{\chi}(\omega) \equiv \frac{\chi(\omega)}{\chi_0} = \int_0^{\infty} d\epsilon \int_0^1 \frac{dp}{p\sqrt{1-p}} \ln^2\left(\frac{\tilde{J}}{\epsilon\sqrt{p}}\right) \times [p\chi_{xx}(\omega) + (1-p)\chi_{zz}(\omega)], \quad (\text{A7})$$

where $\chi_0 = \pi e^4 g^2 \xi^3 kT/2\varepsilon_s$, $\epsilon = E/kT$, and $\tilde{J} = J/kT \gg 1$.

The following analysis will be based on Eq. (A7). It can be easily shown that under the conditions of the present experiment the only important contribution to the dissipative part of the susceptibility, $\text{Im}\tilde{\chi}(\omega)$, is the one coming from the relaxational mechanism χ_{zz} . Thus we have,

$$\text{Im}\tilde{\chi}(\omega) = \int_0^{\infty} \frac{d\epsilon}{\cosh^2(\epsilon/2)} \int_0^1 \frac{dp\sqrt{1-p}}{p} \times \ln^2\left(\frac{\tilde{J}}{\epsilon\sqrt{p}}\right) \frac{\gamma_{\parallel}\omega}{\omega^2 + \gamma_{\parallel}^2}. \quad (\text{A8})$$

An important feature of the relaxation rate γ_{\parallel} is that $\gamma_{\parallel}(\epsilon, p) = p\gamma_0(\epsilon)$, see e.g., Ref. 15. Since we are interested in the case $\omega \ll \gamma_0$, we can put $\epsilon = 1$, $p = p_{\omega} \equiv \sqrt{\gamma_0(1/\omega)}$ in the argument of the logarithm and take the logarithm out of the integrand. As a result,

$$\text{Im}\tilde{\chi} = \pi \left(\mathcal{L}_T + \frac{1}{2}\mathcal{L}_{\omega} \right)^2, \quad (\text{A9})$$

where $\mathcal{L}_T = \ln\tilde{J} \gg 1$ while $\mathcal{L}_{\omega} = \ln(1/p_{\omega}) \gg 1$.

The relaxational contribution to the real part can be written as

$$\begin{aligned} \text{Re}\tilde{\chi}_{zz}(\omega) &= \int_0^{\infty} \frac{d\epsilon}{\cosh^2(\epsilon/2)} \int_0^1 \frac{dp\sqrt{1-p}}{p} \\ &\times \ln^2\left(\frac{\tilde{J}}{\epsilon\sqrt{p}}\right) \frac{\gamma_{\parallel}^2}{\omega^2 + \gamma_{\parallel}^2} \\ &\approx 2 \int_{p_{\omega}}^1 \frac{dp}{p} \left(\mathcal{L}_T - \frac{1}{2} \ln p \right)^2 \\ &= 2\mathcal{L}_{\omega} \left(\mathcal{L}_T^2 + \frac{1}{2}\mathcal{L}_T\mathcal{L}_{\omega} + \frac{1}{12}\mathcal{L}_{\omega}^2 \right). \end{aligned} \quad (\text{A10})$$

The contribution from χ_{xx} to the real part of the susceptibility is also important. Putting $\hbar\omega \ll E$ we obtain

$$\begin{aligned} \text{Re}\tilde{\chi}_{xx} &= 2 \int_0^{\infty} \frac{d\epsilon}{\epsilon} \tanh(\epsilon/2) \int_0^1 \frac{dp}{\sqrt{1-p}} \ln^2\left(\frac{\tilde{J}}{\epsilon\sqrt{p}}\right) \\ &\approx 4\mathcal{L}_T^2 \int_0^{\infty} \frac{d\epsilon}{\epsilon} \tanh\left(\frac{\epsilon}{2}\right). \end{aligned} \quad (\text{A11})$$

The last integral diverges logarithmically at its upper limit. That means that the result is substantially dependent on the total structure of the impurity band. Assuming that (i) $e^2/\varepsilon_s \xi \mathcal{L}_T \ll \hbar \omega_c$, and (ii) that we are interested in the situation when the Fermi level is in the middle of the gap, we can replace for a *very crude* estimate

$$g^2 \int_0^\infty \frac{d\epsilon}{\epsilon} \tanh\left(\frac{\epsilon}{2}\right) \text{ by } \int_0^\infty \frac{d\epsilon}{\epsilon} g^2(\epsilon) \tanh\left(\frac{\epsilon}{2}\right).$$

According to certain experimental evidence, the density of localized states within the gap is a weak function of the energy. Then an estimate for the above integral can be written as $c g^2 \mathcal{L}_c$, where $\mathcal{L}_c = \ln(\hbar \omega_c / kT)$, while $c \geq 1$ is a correction factor due to energy dependence of the density-of-states. As a result, we obtain

$$\text{Re } \tilde{\chi}_{xx} \approx 4c \mathcal{L}_T^2 \mathcal{L}_c. \quad (\text{A12})$$

Since $\text{Re } \sigma / \text{Im } \sigma = \text{Im } \chi / \text{Re } \chi$ we obtain Eq. (10).

-
- ¹D. Weiss, K.v. Klitzing, and V. Mosser, in *Two Dimensional Systems: Physics and New Devices*, edited by G. Bauer, F. Kuchar, and F. Heinrich (Springer-Verlag, Berlin, 1986).
- ²M. Furlan, Phys. Rev. B **57**, 14 818 (1998).
- ³M.V. Gavrilov and I.V. Kukushkin, Pis'ma Zh. Éksp. Teor. Fiz. **43**, 79 (1986) [JETP Lett. **43**, 103 (1986)].
- ⁴F. Tremblay, M. Pepper, R. Newbury, D.A. Ritche, D.C. Peacock, J.E.F. Frost, G.A.C. Jones, and G. Hill, J. Phys.: Condens. Matter **2**, 7367 (1990).
- ⁵F.W. VanKeuls, X.L. Xu, H.W. Jiang, and A.J. Dahm, Phys. Rev. B **56**, 1161 (1997).
- ⁶S.I. Khondaker, I.S. Shlimak, J.T. Nicholls, M. Pepper, and D.A. Ritche, *Proceedings of the 24th International Conference on the Physics of Semiconductors, Jerusalem, Israel*, edited by D. Gershoni (World Scientific, Singapore, 1998) on CD-ROM.
- ⁷I.L. Drichko, A.M. D'yakonov, I.Yu. Smirnov, V.V. Preobrazhenskii, and A.I. Toropov, Semiconductors **33**, 892 (1999).
- ⁸V.D. Kagan, Semiconductors **31**, 470 (1997).
- ⁹I.L. Drichko and I.Yu. Smirnov, Semiconductors **31**, 933 (1997).
- ¹⁰A. Wixforth, J.P. Kotthaus, and G. Weimann, Phys. Rev. Lett. **56**, 2104 (1986); A. Schenstrom, Y.J. Quian, M.F. Xu, H.P. Baum, H. Levy, and B.K. Sarma, Solid State Commun. **65**, 739 (1988).
- ¹¹I.L. Drichko, A.M. D'yakonov, A.M. Kreshchuk, T.A. Polyanskaya, I.G. Savel'ev, I.Yu. Smirnov, and A.V. Suslov, Semiconductors **31**, 384 (1997).
- ¹²I.L. Drichko, A.M. D'yakonov, V.D. Kagan, I.Yu. Smirnov, and A. I. Toropov, *Proceedings of the 24th International Conference on the Physics of Semiconductors, Jerusalem, Israel*, edited by D. Gershoni (World Scientific, Singapore, 1998) on CD-ROM.
- ¹³A.L. Efros, Zh. Éksp. Teor. Fiz. **89**, 1834 (1985) [Sov. Phys. JETP **62**, 1057 (1985)].
- ¹⁴A.L. Efros and B.I. Shklovskii, in *Electron-Electron Interactions in Disordered Systems*, edited by A.L. Efros and M. Pollak (North-Holland, Amsterdam, 1985), p. 409. See also more recent paper D.G. Polyakov and B.I. Shklovskii, Phys. Rev. B **48**, 11 167 (1993) where the case of quantum Hall effect is considered.
- ¹⁵Yu.M. Galperin, V.L. Gurevich, and D.A. Parshin, in *Hopping Transport in Solids*, edited by B. Shklovskii and M. Pollak (Elsevier, New York, 1991).
- ¹⁶S.V. Maleev, Zh. Éksp. Teor. Fiz. **84**, 260 (1983) [Sov. Phys. JETP **57**, 149 (1983)].